Memo No. 134

ngVLA Pointing and Primary Beam Requirements given Image Dynamic Range Requirements

Preshanth Jagannathan,[1] T.K. Sridharan,[2] Kumar Golap,[1] and Sanjay Bhatnagar[1]

[1]*NRAO, 1003 Lopezville Road, Socorro, NM, 87801*
[2]*NRAO, 520 Edgemont Road, Charlottesville, VA, 22903*

ABSTRACT

We analyze the imaging limitations introduced due to pointing offsets of the antenna far-field voltage patterns and examine the need for advanced imaging algorithms to achieve the proposed key science goals (KSGs) of the ngVLA. We consider use cases that require high dynamic range (DR) imaging and examine how much error is introduced in the image, impacting the imaging dynamic range, by the expected range of pointing errors. We examine the feasibility of deploying algorithms such as pointing self-calibration as the strategy to achieve equivalent pointing performance to attain the required DR requirements. We also discuss primary beam requirements necessary to meet the image DR requirements.

1. INTRODUCTION

The image quality achieved with an interferometer is quantified in terms of an effective image sensitivity (rms), achievable dynamic range (ratio of peak source flux density to rms; ngVLA adopts the less stringent quadrature sum of image flux to rms ratio) and fidelity (where the sky model is well known). In this memo we will analyze the imaging limitations introduced due to pointing offsets of the antenna far field voltage patterns and examine the need for advanced imaging algorithms to achieve the proposed key science goals (KSGs) of the ngVLA. The requirements on the primary beam used in such advanced algorithms is also discussed.

2. ANTENNA POINTING AND IMAGE DYNAMIC RANGE

Antenna pointing varies with time and errors in the pointing location are introduced by both systematic effects (e.g. pointing model inaccuracy, refraction correction, steady wind and thermal effects) and random statistical errors (e.g. fluctuating wind component, residual servo errors). Although systematic effects are mitigated by performing pointing calibration scans at regular intervals, the residual stochastic errors will still persist. If we approximate the antenna voltage beams of the two antennas on a baseline to be Gaussians, then we can examine the effects of residual pointing errors analytically. The fractional error on the primary beam of a single baseline (i.e. the product of the antenna primary beams) due to pointing error on one antenna, and therefore on the visibility, is

represented as

$$\epsilon \approx 1 - e^{-4ln2((\alpha+\kappa\beta)^2-\alpha^2)} \tag{1}$$

where ϵ is the error in the antenna PB due to the presence of pointing errors, $\alpha = \theta/\text{HPBW}$ is the beam offset position within the primary beam in units of the voltage beam HPBW, $\beta = \sigma_2/\text{HPBW}$ is the pointing error in units of the voltage beam HPBW and κ accounts for the relative orientation of α and β with a worst case value of 1. Without loss of generality, we use this 1D equation to talk about the 2D pointing error of the antenna primary beam, *for the worst case*. The measured pointing offset σ_2 is the mean of a Rayleigh distribution arising from tracking with two assumed independent axes, each characterized in 1D by zero-mean and normally distributed tracking error σ. Even though the amplitude error expression in (1) is per baseline, there are only N_{ant} number of independent voltage beams and consequently the error on the image constructed from data from an N_{ant} array would be expected to scale as $\sqrt{N_{ant}}$, i.e. $\epsilon_{eff} = \epsilon/\sqrt{N_{ant}}$ (Sridharan et al. (2023)). Finally, ignoring phase variations over the primary beam (which are included in the mitigation strategy proposed in Section 4), we determine the effective image dynamic range as the inverse of this effective fractional error, which is represented as

$$DR = \frac{1}{\epsilon_{eff}} = \frac{\sqrt{N_{ant}}}{\epsilon} \tag{2}$$

3. NGVLA HIGH DYNAMIC RANGE USE CASES

We consider use cases that require high dynamic range (DR) imaging and examine how much error is introduced in the image, impacting the imaging dynamic range, by the expected range of pointing errors, given

1. The known best achievable pointing accuracy floor of 1.2" (per mtex prototype antenna error budget sheet; Selina, Mangum, private communications), in the absence of wind and other external factors

2. A rule-of-thumb pointing accuracy of 3", derived as better than $< 1/10$ HPBW at 115 GHz, under conditions prescribed as *precision conditions* for the ngVLA.

3. The theoretical pointing specification needed to achieve the ngVLA dynamic range requirements

If the theoretical pointing specification is much more stringent than the precision pointing accuracy then we need to examine the feasibility of utilizing algorithms such as pointing self-calibration to achieve the DR required by the applicable KSGs.

Two KSGs driving the requirements for high dynamic range wide-field imaging are the focus of this analysis (resulting in the DR system requirement SYS6103). The first KSG of relevance to this study is a single pointing deep field observation at 8 GHz with an effective sensitivity of 0.035 μJy and an effective dynamic range of 45 dB (31623:1) across the antenna primary beam. The second is a mosaicked observation at 27 GHz providing 35 dB (3162:1) DR across the mosaic response.

3.1. *Single Pointing Deep Field Imaging*

For the ideal pointing case of 1.2", we fall short of the 45 dB DR requirement at 8 GHz due to pointing errors as seen in Fig. 1 and Table 1. As the ideal case represents the absolute pointing error floor, it will only be available exceedingly rarely, if at all. Only a 3" performance is expected in the

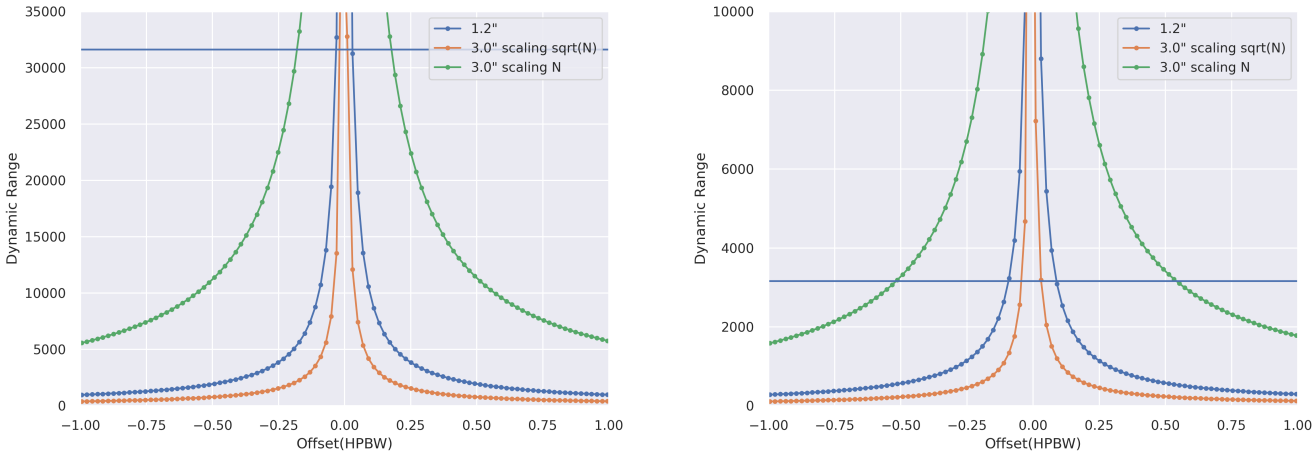

Figure 1. Plotted are curves for the expected dynamic ranges given pointing errors of 1.2" (ideal) and 3.0" (precision conditions), with a $\sqrt{N_{ant}}$ scaling and an aggressive N_{ant} scaling (green) at 8 GHz (left panel) and 27 GHz (right panel). The offset positions within the primary beam (x-axis) are given in units of the HPBW of the power beam and the curves are calculated assuming $N_{ant} = 214$. The horizontal lines correspond to the DR requirement 45 dB for the panel on the left and 35 dB for the panel on the right.

precision observing conditions under which ngVLA observations with the most stringent requirements will be carried out. The figures include horizontal lines at the requisite DRs which are achievable only across a narrow region around the center of the beam even for the best case windless pointing accuracy case (blue curve) and an even narrower region for the precision condition pointing accuracy (orange curve). Scaling with the number of antennas as $\sqrt{N_{ant}}$ and N_{ant} are shown. Sridharan et al (2023) have shown that a $\sqrt{N_{ant}}$ scaling is expected which should be adopted for deriving the pointing requirements, as opposed to an aggressive N_{ant} scaling. As can be seen in the figure, even with an aggressive N_{ant} scaling, the required 45 dB DR is only met over a quarter of the the primary beam. The values of the DR for different representative offset locations within the primary beam are also shown in Table 1. Following this analysis, we derive the pointing specification required to achieve the 45 dB DR all across the HPBW at 8 GHz is 0.07" for an array containing 214 antennas and 0.05" for an array of 107 antennas. The gain in DR by averaging multiple snapshots with independent pointing errors is not considered in these estimates to allow for attainment of high dynamic ranges in short observations, as the DR requirements are general and not restricted to long observations. This establishes a clear need to analyze the feasibility of algorithms such as pointing self-calibration Bhatnagar & Cornwell (2017) to see if the KSG DRs are achievable despite the mechanical pointing limitations of the array.

3.2. *Antenna Pointing Errors and Mosaics*

The second KSG requiring high DR is mosaic imaging at 27 GHz. Assuming a hexagonal mosaic pattern, the pointing centers are separated by a distance of HPBW/$\sqrt{2}$. The dynamic range specification for the mosaicked observation is given to be 35dB (3162:1) at 27 GHz. In order to understand the effects of mosaicking, a hexagonal mosaic was generated around the nominal source of interest as required by the KSG. For this particular analysis we used the simulated galaxy image of NGC 5713

Table 1. The table contains the DR range limits calculated for the KSG requiring deep widefield imaging at 8 GHz and 27 GHz assuming $N_{ant} = 214$, over the primary beam. The offset positions are specified in units of HPBW of the power beam.

Offset (HPBW)	Pointing (arcsec)	DR (8 GHz) (dB)	DR(27 GHz) (dB)
0.1	3	38.7	33.1
0.4	3	32.8	27.5
1.0	3	28.9	23.7
0.1	1.2	42.8	38.7
0.4	1.2	36.8	32.8
1.0	1.2	32.9	28.9

shown in Fig. 2 (Murphy, private communication), which formed the basis for the 35 dB requirement. The hexagonal mosaicking pattern generated is displayed in the left panel of Fig. 3.

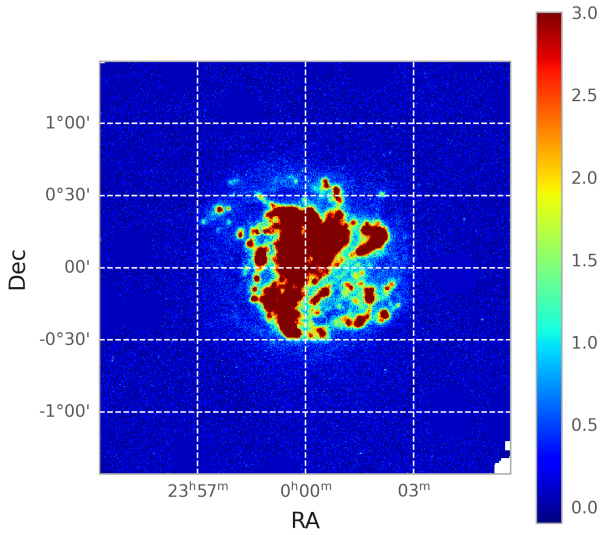

Figure 2. The figure shows the 27 GHz model continuum image achieving a sensitivity of 2 μJy across the image (Murphy, private communication). The peak emission per pixel from this simulation is 40 μJy. The DR is computed following the recommendation of summing the emission in quadrature and taking the ratio with respect to the noise as is more appropriate for extended sources (Murphy (2023)). In that case the sum of the flux in quadrature exceeds $7mJy$ pushing the DR per pointing to over 35 dB.

To figure out the amplitude error in the reconstruction arising purely from a PB pointing offset, we constructed a mosaic where each of the 7 pointings (6 hexagonal vertices and 1 central) in the hexagonal mosaic are offset in multiple random directions to generate an offset error map. However, the maximum error occurs when the pointings are each offset by the maximum pointing offset along the direction of the pointing phase center with respect to the mosaic center. To produce the worst case error map each of the pointing centers was offset by 3", the precision conditions pointing offset value, along the vector from the mosaic center to the pointing phase center, to derive the mosaic

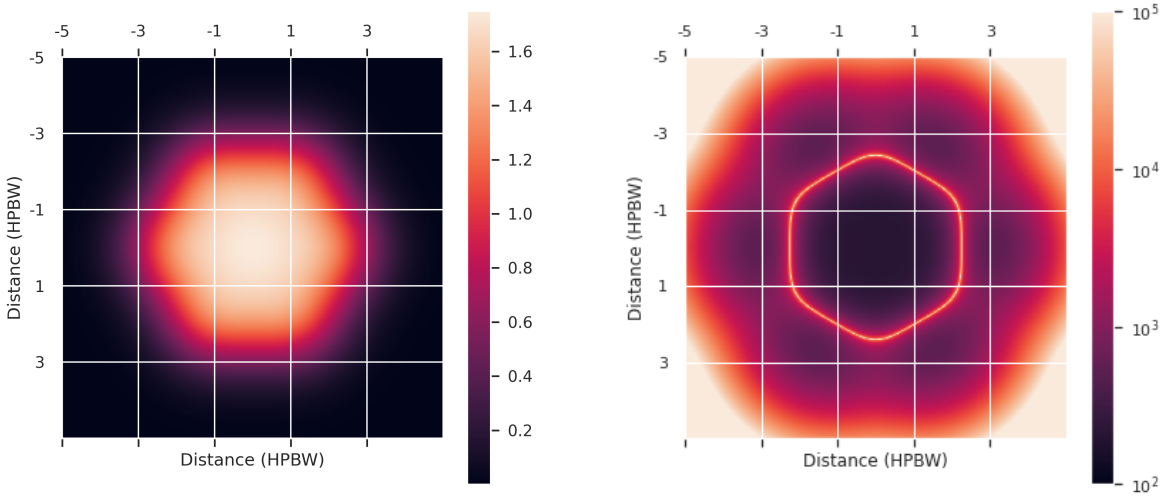

Figure 3. Plotted in the left panel is the mosaic sensitivity at 27 GHz. Plotted in the right panels is the DR of the mosaic with an offset of 1.2", the windless pointing error specification that falls short of the DR requirement across the FoV.

which we will call the perturbed hexagonal mosaic. This provides the worst case scenario in terms of the pointing performance. We compute a nominal error in the reconstruction by constructing an error map represented by the difference of the true mosaic response with the perturbed hexagonal mosaic. The error map is subsequently turned into a dynamic range by means of eqn. 2. The dynamic range map is shown in the right panel of Fig. 3. The estimated dynamic range around the central region of the mosaic ranges from 27 dB (500:1) to about 30 dB (1000:1). The requirement to achieve the proposed KSG is 35 dB and we fall short of that. To achieve the desired dynamic range of 35 dB, the analysis reveals that the pointing error must be less than 0.18" for a $N_{ant} = 214$ and less than 0.13" for a $N_{ant} = 107$ during the mosaicked observation. These limits are derived numerically by computing the maximum possible error for the observation i.e. the normalized difference of the perturbed beam observation and an ideal observation, including the thermal noise across a hexagonal mosaic. The dynamic range is derived as described by Eqn. 2.

4. POINTING SELF-CALIBRATION (PSC)

As presented above, the DR requirements at 8 GHz and 27 GHz cannot be met by the level of mechanical pointing performance expected to be achieved by the ngVLA antennas, based on information from the ongoing prototype antenna development effort. Therefore, other approaches are needed and we propose pointing self-calibration (PSC) as the strategy to deliver the required effective high pointing performance.

Pointing self-calibration is a direction dependent calibration that calculates the gain (amplitude and phase) of the antennas due to a pointing offset and is carried out iteratively utilizing a model image generated at the time of imaging (hence Self-calibration). The details of the algorithmic implementation and successful tests on the VLA are presented in Bhatnagar & Cornwell (2017). In order decide if pointing self-calibration is indeed feasible, we need to determine the minimum

solution interval across which there is sufficient SNR to derive solutions. Pointing self-calibration uses information across the entire field of view (FoV), consequently the sources across the FoV that will show up in the solution interval are used. This predicates the need for emission across the PB if one is to be able to calculate the offsets over shorter solution intervals. Now consider the equation for the SNR of the pointing solution interval Bhatnagar & Cornwell (2017)

$$SNR_{psc} = \frac{\nabla S}{SEFD}\sqrt{\delta\nu_{sol}\tau_{sol}(N_{ant}-1)} \tag{3}$$

where SNR_{psc} gives the SNR per pointing selfcal solution interval and ∇S gives the apparent flux gradient in the antenna PB and SEFD is the sensitivity of the instrument, $\delta\nu_{sol}$ is the effective bandwidth over which the solution is derived, and τ_{sol} is the time interval of averaging to derive the pointing solution. The apparent flux gradient is given by,

$$\nabla S = \int \left(\frac{\partial E}{\partial l} \otimes E^{*}\right) I^{M}(s) ds \tag{4}$$

Eqn. 3 can be inverted to determine the time interval in seconds over which a solution can be determined given SNR_{psc} as

$$\tau_{sol} = \left[\frac{SNR_{psc} * SEFD}{\nabla S}\right]^{2} \frac{1}{\delta\nu_{sol}(N_{ant}-1)} \tag{5}$$

If we assume Band 2 parameters i.e. $SEFD = 264.8$ Jy, and $\nabla S \approx 20$ mJy/arcsec, from source counts derived from the recent MeerKAT Absorption Line Survey (Deka et al. 2023),we scale the fluxes from 1.4GHz to 8GHz assuming a mean spectral index of -0.7, we determine that the deep field will nominally contain a set of point sources spread across the primary beam. The point source distribution is multiplied by the derivative of the PB given a pointing offset error requirement of 0.07" (refer to sec. 3.2), which provides an estimate of ∇S given by eqn. 4. For a bandwidth of 8 GHz and number of antennas as $N_{ant} = 214$ for an effective $SNR_{psc} = 3$ we derive the effective time on source required to derive a usable pointing solution interval to be $\tau_{sol} = 2$ seconds. For the mosaic, for a pointing offset error of 0.18" (refer to sec. 3.2) the flux gradient per pointing is given by $\nabla S \approx 680\mu$Jy/arcsec, derived by applying the derivative of the pointing (similar to right panel of Fig. 3 but with a pointing offset per pointing of 0.18") along with the mosaicked voltage pattern. To derive the gradients for the single pointing and mosaic cases, the product of derivative of the antenna Jones and its derivative (see Fig. 3) are obtained. This is multiplied by a model image and summed to obtain ∇S. In order to determine the flux in a model image at X-Band for the Band 2 KSG we utilized the source counts curve from the MeerKAT Absorption Line Survey Deka et al. (2023). In the Mosaic KSG the image shown in Fig. 2 was used. The required 35 dB DR results in a solution interval of $\tau = 2.3$ s for $N_{ant} = 214$ ($\tau = 4.6$ s for $N_{ant} = 107$) across the full 13.5 GHz instantaneous bandwidth proposed for the nominal pointing offset error of 0.18". It is worth noting that a smaller pointing offset requires more sources to attain solutions of the same SNR and a more perfect knowledge of the beam.

The estimates derived here provide a more stringent effective pointing performance than the best achievable pointing accuracy floor of 1.2". In other words, statistical pointing variations occurring on time scales as short as a few to several seconds due to fluctuating wind conditions and residual servo

performance errors can be corrected for using pointing self-calibration. This is yet another illustration of the impressive sensitivity of the ngVLA, which allows for the implementation of advanced calibration methods to meet the scientific goals. This approach mirrors previous studies that have highlighted self-calibration as a powerful technique available for ngVLA (Sridharan & Bhatnagar (2023)).

The theoretical models and analysis presented above provide the basis for the viability of deploying pointing self-calibration methods as the strategy to achieve stringent equivalent pointing performance necessary to attain the high ngVLA dynamic range requirements. More careful simulations on ngVLA scale, incorporating detailed complex antenna electric field patterns and their derivatives are needed to validate the predictions and refine the error margins based on the empirical source flux distributions used in this analysis.

5. PRIMARY BEAM

The antenna primary beam (PB) or the antenna far field voltage pattern is also a sampling function of the sky brightness that is unique to each antenna of an interferometer. Its variation over the array, time and frequency will lead to visibility errors and in turn impact the dynamic range of the constructed images. The dependence of the primary beam (PB) of an individual baseline over time and frequency provides the starting point for the analysis of tolerance in the knowledge of primary beams. Following the prescription laid out in Bhatnagar et al. (2013) we can make the case that any discrepancy in the knowledge of the antenna PB directly results in errors both in deconvolution and in flux scaling, and therefore image errors and dynamic range limitations. To analyze the contribution of errors from the PB in deconvolution requires detailed simulations which are beyond the scope of the current work. The PB flux scaling error however skews in line with the errors arising from pointing offsets. At this juncture we will relax a couple of our prior assumptions i.e. the beam is both chromatic and time varying, where the variation in time is a field rotation as the antennas are on altitude azimuth mounts. Revisiting the antenna equation for the apparent sky brightness as seen by an individual baseline of an interferometer.

$$I_{ij}^{obs} = \sum_{\nu} \sum_{t} (J_i \otimes J_j^*) S_{ij} * I^{True} \tag{6}$$

Where I_{ij}^{obs} is the observed apparent sky brightness as seen by the antennas of the baseline ij, S_{ij} is the Fourier transform of the sampling function in the UV introduced by the baseline. The term $(J_i \otimes J_j^*)$ makes clear the role of the Jones matrices (voltage units): J_i and J_j are (include) the antenna voltage beam patterns, resulting in the baseline power pattern given by their outer product, as an additional imprint on the overall measurement (Jagannathan (2018)). In order to achieve the proposed dynamic range of 45 dB at 8 GHz it is required that the product of these Jones matrices averaged over time and frequency be known to a better level, by 1.5 dB, than the DR since the errors in the primary beam knowledge will add in quadrature with the thermal noise required to achieve the 45 dB DR at 8 GHz across the band.

In the voltage measurement of an individual antenna i, the voltage pattern is given by

$$V_i^m = V_i + \epsilon_i \tag{7}$$

where V_i^m is the measured or model antenna voltage pattern which is the summation of the true voltage pattern V_i and the error in the measurement given by ϵ_i. For a baseline of antennas i and j

it results in

$$P_{ij} = (V_i * V_j) + \epsilon_{ij} \tag{8}$$

The allowable noise (error) $\epsilon_{ij} = \sqrt{\epsilon_i^2 + \epsilon_j^2}$ for a baseline comes from the DR requirement of 45 dB at 8 GHz and scales as $1/\sqrt{N}$ as given by Sridharan et al. (2023). Assuming $N_{ant} = 214$ antennas the DR per baseline is 33.3 dB, or 34.8 dB for $N_{ant} = 107$. This error per baseline can be translated to the error per antenna assuming uniform sensitivity across the antennas of a baseline and independent errors. Since the baseline error is in visibility domain (units of power) and the per-antenna error is in voltage, the per-antenna voltage beam DR requirement is 31.8 dB for $N_{ant} = 214$ or 33.3 dB for $N_{ant} = 107$. The corresponding per-antenna power beam DR requirement would be 3 dB higher (34.8 dB for $N_{ant} = 214$ or 36.3 dB for $N_{ant} = 107$) due to error propagation when going from voltage to power.

Extending the analysis to the requirement of 35 dB at 27 GHz then results in a per baseline DR of 23.3 dB for $N_{ant} = 214$ or 24.8 dB for $N_{ant} = 107$. Once again assuming the antennas are alike and similarly illuminated and independent errors, we get a per-antenna voltage beam DR requirement of 21.8 dB for $N_{ant} = 214$ and 23.3 dB for $N_{ant} = 107$. The corresponding per-antenna power beam DR requirement would be 24.8 dB for $N_{ant} = 214$ or 26.3 dB for $N_{ant} = 107$. The single pointing case is considered as it provides a more stringent requirement. When mosaicked there is an additional gain in DR arising from the improved sensitivity based on the mosaicking strategy employed. For a hexagonal mosaic the DR improves by a factor of $\sqrt{3}/2$ corresponding to the increased sensitivity.

The error limits specified here are for PB variations over the array, time and frequency and the algorithm for PB error correction will be A-projection. Errors common to all antennas and therefore to all visibilities, will impact image fidelity for which the requirement is a lot less stringent ($> 0.9 \sim$ 10 dB; SYS6107, SYS6108) than dynamic range. The variation with frequency is addressed in more detail in the next section.

5.1. *PB channelization limits to meet fidelity requirements.*

This section examines the impact of PB and visibility data channelization on achieving the ngVLA imaging fidelity requirement, specifically focusing on the accuracy of amplitude corrections across frequency. The goal is to determine the maximum tolerable error in the PB's frequency response to maintain the necessary amplitude accuracy to deliver the fidelity requirement of > 0.9 (i.e. 10 dB).

The channelization width of the PB is critical in A-projection and PSC because these techniques apply frequency-dependent corrections to account for the PB's variation across the observed bandwidth. Insufficient channelization can lead to inaccurate PB modeling, particularly when dealing with wide-field imaging across wide bandwidths. Broad channels can cause significant errors because the PB's shape and gain change appreciably within the frequency channel extent, leading to inaccurate corrections. This is distinct from bandwidth smearing of visibilities, which is a separate effect.

To derive the requirement, we can consider the error introduced at the edges of some frequency range we choose to correct for the beam through A-projection, using the beam at the center of the range. The FWHM of the antenna primary beam is given by λ/D or with frequency as $c/\nu D$ where c is the speed of light, ν is the frequency and λ is the wavelength of incident radio waves.

We assume a Gaussian main lobe approximation of the power beam to estimate the resulting errors analytically. The use of the power beam is appropriate here because channelization errors affect all

antennas equally, this is a systematic error due to using the channel-center beam pattern, which is in error at channel edges by the same amount for all antennas.

We can determine the standard deviation from the FWHM of the antenna power beam as:

$$\sigma_\nu = \frac{c}{\nu D \times 2\sqrt{2\ln 2}} \tag{9}$$

The fractional error $\epsilon_{PB}(\nu)$ in the power beam can be obtained by finding the maximum difference between the beam at the channel center and at the channel edge, normalized by the beam response at the channel center:

$$\epsilon_{PB} = \frac{\left| e^{-\frac{x^2}{2\sigma_0^2}} - e^{-\frac{x^2}{2\sigma_1^2}} \right|}{e^{-\frac{x^2}{2\sigma_0^2}}} \leq 1 - \mathcal{F} \tag{10}$$

where $\sigma_0 = \sigma(\nu_0)$, $\sigma_1 = \sigma(\nu_0 + \delta\nu/2)$.

We solve Equation 10 numerically by finding the x position for the maximum of $\epsilon_{PB}(\nu)$ and determine the channel width $\delta\nu$ that satisfies the fidelity requirement $\mathcal{F} = 0.9$. As the error we are considering is a systematic effect it will also not scale down with the number of antennas. The results are shown in Table 2.

Band	Freq Start (GHz)	Channel Width (MHz)
1	1.2	25
2	3.2	68
3	12.3	264
4	20.5	441
5	30.5	656
6	70.0	1506

Table 2. Derived minimum channel width for each band at the lowest frequency of the band where the error is maximal. The computation finds the maximum fractional error using Equations 9 and 10 to achieve the fidelity specification of 0.9.

6. SUMMARY

This memo has presented an analysis of the imaging limitations imposed by antenna pointing errors and primary beam (PB) uncertainties on achieving the dynamic range (DR) and image fidelity requirements of the ngVLA. We derive specific technical requirements for mechanical antenna pointing, the application of pointing self-calibration, and the necessary tolerances in primary beam knowledge and channelization.

The key conclusions from the analysis are:

- **Antenna Pointing Performance Gap:** The effective image dynamic range is directly impacted by pointing errors, conservatively scaling as $DR = \sqrt{N_{ant}}/\epsilon$. To meet the 45 dB DR requirement at 8 GHz across the antenna HPBW, a theoretical pointing specification of 0.07" (for $N_{ant} = 214$) or 0.05" (for $N_{ant} = 107$) is required. This is significantly more stringent

than the expected best achievable mechanical pointing accuracy floor of 1.2" and the precision condition pointing accuracy of 3". Similarly, for 35 dB DR mosaicked observations at 27 GHz, the pointing error must be less than 0.18" (for $N_{ant} = 214$) or 0.13" (for $N_{ant} = 107$).

- **Pointing Self-Calibration as Essential Strategy:** Given the gap between the expected mechanical pointing performance and requirements, pointing self-calibration is identified as an essential strategy to achieve the effective pointing performance required to fulfill the ngVLA's stringent DR goals. The analysis demonstrates that usable pointing solutions can be obtained with approximately 2 second of integration time at 8 GHz and 2.3 seconds at 27 GHz (for $N_{ant} = 214$), making it feasible to correct statistical pointing variations occurring on rapid timescales.

- **Primary Beam Knowledge Requirements:** To achieve the target dynamic ranges, the primary beam knowledge per antenna must correspond to a power beam dynamic range of 34.8 dB (8 GHz, $N_{ant} = 214$) or 24.8 dB (27 GHz, $N_{ant} = 214$) across the main lobe. Additionally, to meet the imaging fidelity requirement (>0.9) across the full primary beam, specific minimum channel widths for PB correction are required, ranging from 25 MHz at 1.2 GHz to 1506 MHz at 70 GHz.

In conclusion, the analysis clearly establishes that advanced calibration techniques, particularly pointing self-calibration and accurate primary beam modeling with appropriate channelization, are indispensable for the ngVLA to achieve its ambitious high dynamic range key science goals, effectively bridging the gap between intrinsic hardware performance and scientific requirements.

REFERENCES

Bhatnagar, S., & Cornwell, T. J. 2017, AJ, 154, 197, doi: 10.3847/1538-3881/aa8f43

Bhatnagar, S., Rau, U., & Golap, K. 2013, ApJ, 770, 91, doi: 10.1088/0004-637X/770/2/91

Deka, P. P., Gupta, N., Jagannathan, P., et al. 2023, arXiv e-prints, arXiv:2308.12347, doi: 10.48550/arXiv.2308.12347

Jagannathan, P. 2018, PhD thesis, University of Cape Town

Murphy, E. J. 2023, ngVLA Memo 113

Sridharan, T. K., & Bhatnagar, S. 2023, ngVLA Memo 108

Sridharan, T. K., Golap, K., Bhatnagar, S., & Myers, S. 2023, ngVLA Memo 107